Age-related changes in the default mode network are more advanced in Alzheimer disease

D.T. Jones, MD
M.M. Machulda, PhD
P. Vemuri, PhD
E.M. McDade, DO
G. Zeng, PhD
M.L. Senjem, MS
J.L. Gunter, PhD
S.A. Przybelski, MS
R.T. Avula, PhD
D.S. Knopman, MD
B.F. Boeve, MD
R.C. Petersen, MD, PhD
C.R. Jack, Jr., MD

Address correspondence and reprint requests to Dr. Clifford R. Jack, Jr., Department of Radiology, Mayo Clinic, 200 First Street SW, Rochester, MN 55905
jack.clifford@mayo.edu

ABSTRACT

Objective: To investigate age-related default mode network (DMN) connectivity in a large cognitively normal elderly cohort and in patients with Alzheimer disease (AD) compared with age-, gender-, and education-matched controls.

Methods: We analyzed task-free–fMRI data with both independent component analysis and seed-based analysis to identify anterior and posterior DMNs. We investigated age-related changes in connectivity in a sample of 341 cognitively normal subjects. We then compared 28 patients with AD with 56 cognitively normal noncarriers of the *APOE* ϵ4 allele matched for age, education, and gender.

Results: The anterior DMN shows age-associated increases and decreases in fontal lobe connectivity, whereas the posterior DMN shows mainly age-associated declines in connectivity throughout. Relative to matched cognitively normal controls, subjects with AD display an accelerated pattern of the age-associated changes described above, except that the declines in frontal lobe connectivity did not reach statistical significance. These changes survive atrophy correction and are correlated with cognitive performance.

Conclusions: The results of this study indicate that the DMN abnormalities observed in patients with AD represent an accelerated aging pattern of connectivity compared with matched controls.
Neurology® 2011;77:1524–1531

GLOSSARY

AD = Alzheimer disease; **aDMN** = anterior default mode network; **ADRC** = Mayo Clinic Alzheimer Disease's Research Center; **CN** = cognitively normal; **DMN** = default mode network; **ICA** = independent component analysis; **ITN** = intrinsic connectivity network; **MCSA** = Mayo Clinic Study of Aging; **PCC** = posterior cingulate cortex; **pDNM** = posterior default mode network; **ROI** = region of interest; **STMS** = Short Test of Mental Status; **TF** = task-free.

Old age is the greatest risk factor for development of Alzheimer disease (AD).[1] Networks of functional connectivity have been identified using task-free (TF)–fMRI and termed intrinsic connectivity networks (ICNs).[2] ICNs demonstrate specific changes related to neurodegenerative illnesses[3] and advancing age.[4–7] Whether age-related changes in ICNs are similar to the AD changes in ICNs is unknown.

The nature of ICN abnormalities in AD is an active area of investigation focused on the default mode network (DMN), which has connectivity patterns that distinguish healthy aging from AD in task-specific[8] and TF-fMRI models.[9]

The aging DMN is characterized by a breakdown of connectivity within its posterior portions and by loss of connectivity between anterior and posterior subnetworks.[5–7] The anterior-to-posterior disconnection is accompanied by global declines in posterior DMN (pDMN) and enhancement of the anterior DMN (aDMN).[7] This leads to reciprocal age-related changes in the pDMN and aDMN.

Given that the disruption of limbic circuitry impairs DMN connectivity[10] and the relationship between age and limbic tangle pathology,[11] we hypothesized that age-related changes in the DMN

Supplemental data at www.neurology.org

Supplemental Data

From the Departments of Neurology (D.T.J., E.M.M., D.S.K., B.F.B., R.C.P.), Psychiatry/Psychology (M.M.M.), Radiology (P.V., G.Z., M.L.S., J.L.G., R.T.A., C.R.J.), and Biomedical Statistic and Informatics (S.A.P.), Mayo Clinic, Rochester, MN.
Study funding: Supported by the NIH (R01-AG11378, P50-AG16574, U01-AG06786), the Alexander Family Alzheimer's Disease Research Professorship of the Mayo Foundation, USA, and Opus building (NIH C06-RR018898).
Disclosure: Author disclosures are provided at the end of the article.

Table 1 Demographics, STMS, and *APOE* status[a]

	CN ϵ4− (n = 56)	AD (n = 28)	*p* Value	Age cohort (n = 341)
Women, n (%)	21 (38)	10 (36)	0.87	141 (41)
APOE ϵ4 carrier, n (%)	0	19 (68)	<0.001	70 (23)[b]
Age, y, median (minimum, maximum)	79 (64, 91)	78 (62, 92)	0.52	82 (60, 94)
Education, y median (minimum, maximum)	14 (8, 20)	16 (8, 20)	0.36	13 (7, 20)
STMS score, median (minimum, maximum)	36 (30, 38)	25 (15, 34)	<0.001	35 (27, 38)

Abbreviations: AD = Alzheimer disease; CN = cognitively normal; STMS = Short Test of Mental Status.
[a] CN ϵ4− subjects were matched 2:1 to the subjects with AD on gender, age, and education. *p* Values for the pairwise comparison of the CN ϵ4− and AD groups are reported. Demographics for the large cohort used in the age analysis (Age cohort) are listed in the final column (at the time of this study, genotyping data were not available for every member of this cohort).
[b] *APOE* genotype information missing for 42 (13%).

will be similar to those seen in AD. To test this hypothesis we performed 2 parallel analyses, which were then compared. We first established a pattern of age-related changes in pDMN and aDMN connectivity in 341 cognitively normal (CN) elderly subjects. We then examined differences in the pDMN and the aDMN between 56 CN noncarriers of the *APOE* ϵ4 allele matched on age, gender, and education to 28 subjects with AD.

METHODS

Participants. CN subjects enrolled in either the Mayo Clinic Alzheimer's Disease Research Center (ADRC) or the Mayo Clinic Study of Aging (MCSA), a prospective, population-based study of randomly selected residents of Olmstead County, Minnesota, who had undergone TF-fMRI were included in the age cohort (n = 341).

CN individuals enrolled either in the ADRC or the MCSA (n = 56) with genotyping data and TF-fMRI available at the time of this study and were noncarriers of the *APOE* ϵ4 allele were randomly selected to be age-, education-, and gender-matched 2:1 to the AD group (table 1).

The details of MCSA subject recruitment and design are included in a previous report.[12] In summary, subjects were diagnosed as CN after in-person evaluations were performed by nurses, physicians, and neuropsychologists, during which they gathered risk factor assessments including structured neurologic examinations with mental status screening and routine neuropsychological evaluation.[12] A final diagnosis for each subject is made during a weekly consensus conference involving all study faculty.

All subjects with AD (n = 28) met the National Institute of Neurological Disorders and Stroke and the Alzheimer Disease's and Related Disorders Association criteria and were participants in the ADRC or MCSA.

Standard protocol approvals, registrations, and patient consents. All participants provided written informed consent for participation. The Mayo Clinic institutional review board approved the study and the consenting processes.

TF-MRI data acquisition and preprocessing. TF-fMRI scans were acquired using a General Electric 3-T Signa HDx scanner (8-channel head coil, gradient echo planar imaging, repetition time = 3,000 msec, echo time = 30 msec, 90° flip angle, slice thickness 3.3 without gap, slices covering the entire brain, and 103 volumes). Subjects were instructed to keep their eyes open during scanning. All TF-fMRI sequences with greater than 3 mm of translational movement or 3° of rotational movement were excluded from analysis. Twelve subjects from the aging cohort were excluded from analysis based on movement parameters. No subjects from the AD group or their 56 matched controls were excluded based on movement parameters.

Preprocessing and data analysis was performed using a combination of the statistical parametric mapping (SPM5) software (Wellcome Department of Cognitive Neurology, University College London, London, UK), the resting-state fMRI data analysis toolkit (www.restfMRI.net),[13] group ICA of fMRI toolbox software,[14] and in-house–developed software implemented in MATLAB (Mathworks Inc., Natick, MA).

Preprocessing steps included discarding of the first 3 volumes, slice time correction, realignment, normalization to SPM5 echo planar imaging template, smoothing with 4-mm full-width at half-maximum Gaussian kernel, linear detrending, and 0.01–0.08 Hz bandpass filtering. In addition, regression correction for spurious variables included rigid body transformation motion effects, global mean signal, white matter signal, and CSF signal.[11,15,16] Removal of global signal by regression improves the specificity of connectivity analysis,[15] and, when directly measured physiologic cardiac and respiratory inputs are not available,[17] it is an attractive method for reducing spurious direct correlations. This is necessary because gray matter has significantly greater capillary density than white matter,[18] and this variability is not accounted for by CSF and white matter regression alone.[15] These preprocessed images were used for both independent component analysis (ICA) and seed-based connectivity analysis.

The structural MRI sequence was a 3-dimensional magnetization-prepared rapid acquisition gradient echo imaging sequence developed for the Alzheimer Disease's Neuroimaging Initiative study.[19]

ICA of the age effect in the CN cohort. The ICNs were first identified using group ICA of fMRI toolbox[14] with a low-dimensional estimation of 20 independent components.[20] The group ICA analysis was run 100 times using the ICASSO function to ensure stability of the 20 estimated components. The DMN was identified by visual inspection of the group independent components for further analysis. Two components were identified, one displaying posterior-dominant DMN connections (i.e., the pDMN) and the other displaying anterior-dominant DMN connections (i.e., the aDMN). The individual subject ICNs were derived using the spatial and temporal dual regression method. Each subject's age was used as a covariate in an SPM linear regression analysis (figure 1) with cluster level correction ($p < 0.05$) to highlight network level dynamics (the SPM-compatible code for cluster level correction is available at http://www2.warwick.ac.uk/fac/sci/statistics/staff/academic-research/nichols/scripts/spm/johnsgems5/CorrClusTh.m).

ICA of AD vs matched control groups. The same ICA procedure outlined above was used to identify the aDMN and pDMN in the AD and matched CN groups. A 2-sample *t* test with cluster-level correction was used to compare aDMN and pDMN components between AD and CN groups ($p < 0.05$). To limit results to within-network changes in connectivity, an inclusive mask of the spatial extent of the CN group DMN under investigation was applied (figure 2).

Conjunction analysis. A conjunction analysis was performed to test the global null hypothesis to identify voxels that displayed

Figure 1 Age effect

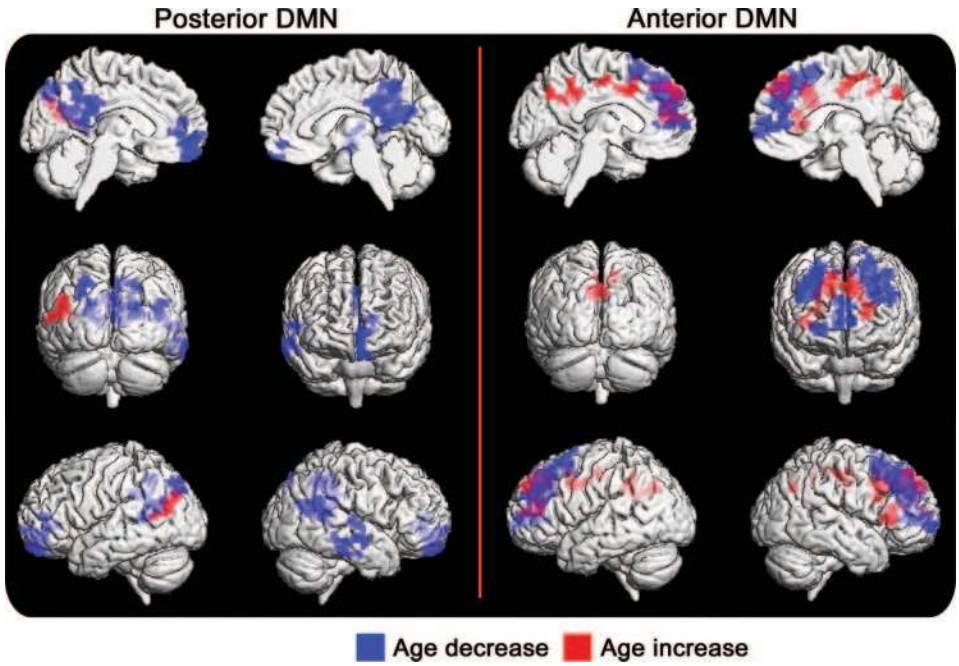

The age effect on the independent component analysis of the posterior (left) and anterior (right) default mode networks (DMNs) in a large cohort of cognitively normal elderly controls. Regions displaying greater connectivity with advancing age are in red, and regions displaying less connectivity with advancing age are in blue (corrected cluster-level $p < 0.05$).

similar behavior in the age regression (n = 341) and the 2-sample *t* test between AD (n = 28) and matched CN (n = 56) groups. This was performed on the back-reconstructed individual components for the pDMN and aDMN. Results were considered significant at a corrected cluster-level $p < 0.05$, with an inclusive mask. All permutations for the conjunction analyses were performed (figure 3).

Seed-based voxel-wise connectivity analysis of AD vs matched control groups. The ICA analysis was used to select the seed regions of interest for the voxel-wise connectivity analysis. The most significant difference between AD and CN groups in the pDMN was located in the precuneus (Montreal Neurologic Institute coordinate −6, −63, 27). The most significant difference between the AD and CN groups in the aDMN was located in the medial prefrontal cortex (Montreal Neurologic Institute coordinate 12, 51, 36). At each of these locations, we placed a 6-mm seed region of interest (ROI). The average blood oxygen level–dependent signal time course within each ROI was correlated to every voxel in the brain for each subject using Pearson correlation coefficients. The correlation coefficients were then converted to *z* scores using the Fisher *r*-to-*z* transformation. A 1-sample *t* test (false discovery rate $p < 0.05$) was used to display the voxel-wise connectivity maps for each of the 2 seeds corresponding to the anterior and posterior DMN group maps (figure 4). A 2-sample *t* test was used to compare group differences in voxel-wise connectivity maps thresholded with cluster-level correction for both the aDMN and pDMN ($p < 0.05$) with an inclusive mask (figure 4). This 2-sample *t* test was then repeated while controlling for connectivity variance accounted for by differences in gray matter density on a voxel-wise basis by entering each subject's gray matter probability maps as a covariate using the Biological Parametric Mapping toolbox.[21]

Correlation with Short Test of Mental Status in AD matched control groups. To investigate the relationship of the voxel-wise connectivity of both the anterior and posterior seeds to cognitive function, we used Short Test of Mental Status (STMS) scores[22] for every subject as a covariate in a linear regression analysis for each group. The result is reported using a corrected cluster level ($p < 0.05$) with an inclusive mask.

RESULTS **Participants.** The 341 (41.3% women) CN subjects included in the age analysis ranged in age from 60 to 94 years (median: 82 years).

A 2-sided Wilcoxon's rank-sum test was used for the continuous variables, and a χ^2 test was used for differences in proportions of gender and *APOE* ϵ4 carrier status. The 56 CN noncarriers of the *APOE* ϵ4 allele did not differ significantly in age, gender, or education from the 28 subjects with AD (table 1). As expected, these 2 groups differed in *APOE* ϵ4 allele carrier status STMS scores ($p < 0.001$).

ICA of the age effect in the CN cohort. Low-dimensional ICA reveals anterior- and posterior-dominant DMN components. The effect of age on the connectivity of the pDMN in the 341 CN subjects shows decreases in connectivity in the posterior cingulate cortex (PCC), precuneus, left inferior parietal lobule, and medial prefrontal cortex and increased connectivity

Figure 2 Alzheimer disease (AD) vs cognitively normal (CN) using independent component analysis

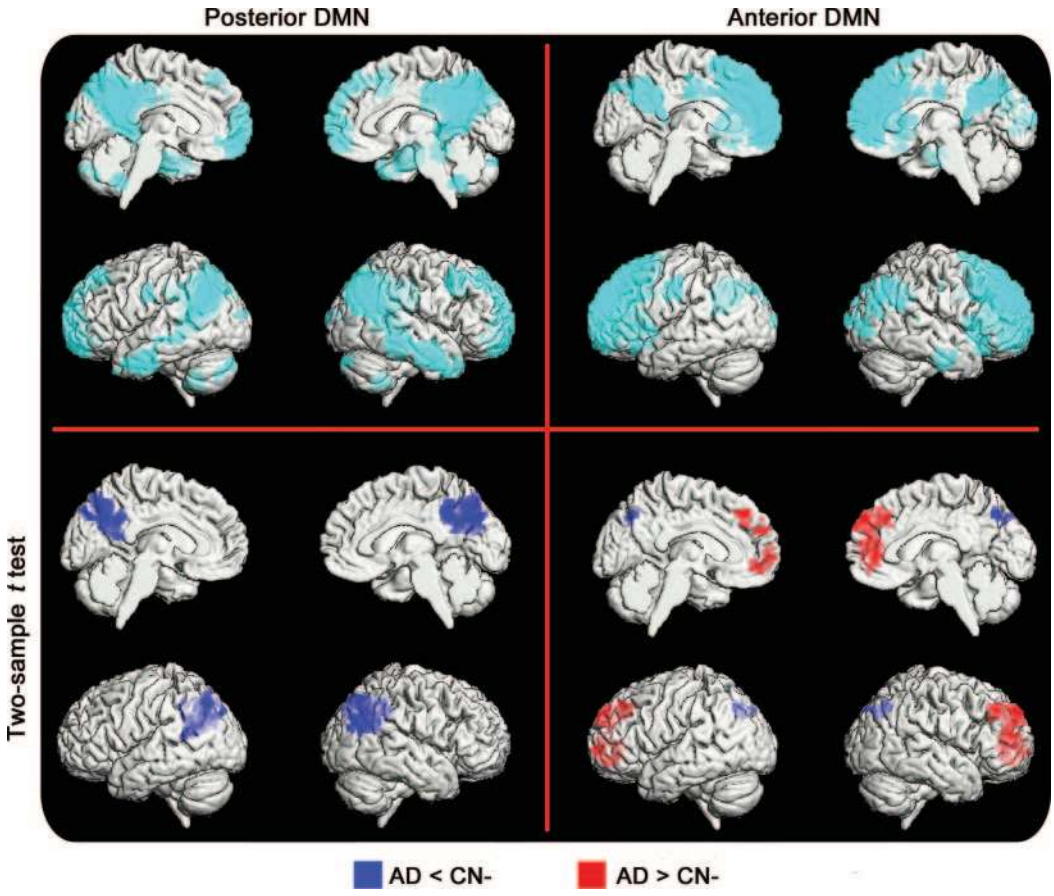

Independent component analysis of posterior (left) and anterior (right) default mode networks (DMNs) in subjects with AD and matched controls. The spatial extent of the anterior DMN and posterior DMN is displayed in the top row (cyan) using a rendering of a 1-sample *t* test for the entire group (false discovery rate–corrected $p < 0.05$). Regions displaying greater connectivity in the AD group are in red, and regions displaying less connectivity in AD are in blue (corrected cluster-level $p < 0.05$).

in the left temporoparietal region, whereas the aDMN displays a combination of increased and decreased connectivity in the frontal lobe with advancing aging. There is also an increase in aDMN connectivity in the retrosplenial PCC with advancing age (figure 1).

ICA of AD vs matched control groups. The group comparison between CN and AD groups reveals a pattern similar to that observed for the age effect (with AD appearing more advanced in age). For the pDMN, the CN subjects display greater connectivity than the subjects with AD in the PCC, precuneus, and left inferior parietal lobule. The AD group does not display any regions of increased connectivity within the pDMN. The same analysis of the aDMN reveals a contrasting pattern. The CN subjects again display a small region of increased connectivity posteriorly, but the subjects with AD display greater connectivity throughout the frontal lobe (figure 2).

Conjunction analysis. The only significant conjunction analyses were between the decreases in connectivity with advancing age and relative decreases in AD within the pDMN and between increases in connectivity with advancing age and relative increases in AD within the aDMN (figure 3 and table e-1 on the *Neurology*® Web site at www.neurology.org). The declines in aDMN connectivity with advancing age were also found in the conjunction analysis with AD < CN, but these did not reach significance.

Seed-based voxel-wise connectivity analysis of AD vs matched control groups. The same analysis on the AD and CN-matched cohorts using seed-based ROI techniques reveals the same pattern as described for the ICA analysis, except the posterior changes in the temporoparietal regions are more left lateralized with an additional involvement of the medial temporal lobe. After assessment for variance related to gray matter density (i.e., atrophy correction), the group differences in the pDMN and aDMN remain significant, including those in the medial temporal regions (figure e-1). However, when variance related to gray matter density is accounted for, the statistical power

Figure 3 Conjunction analysis

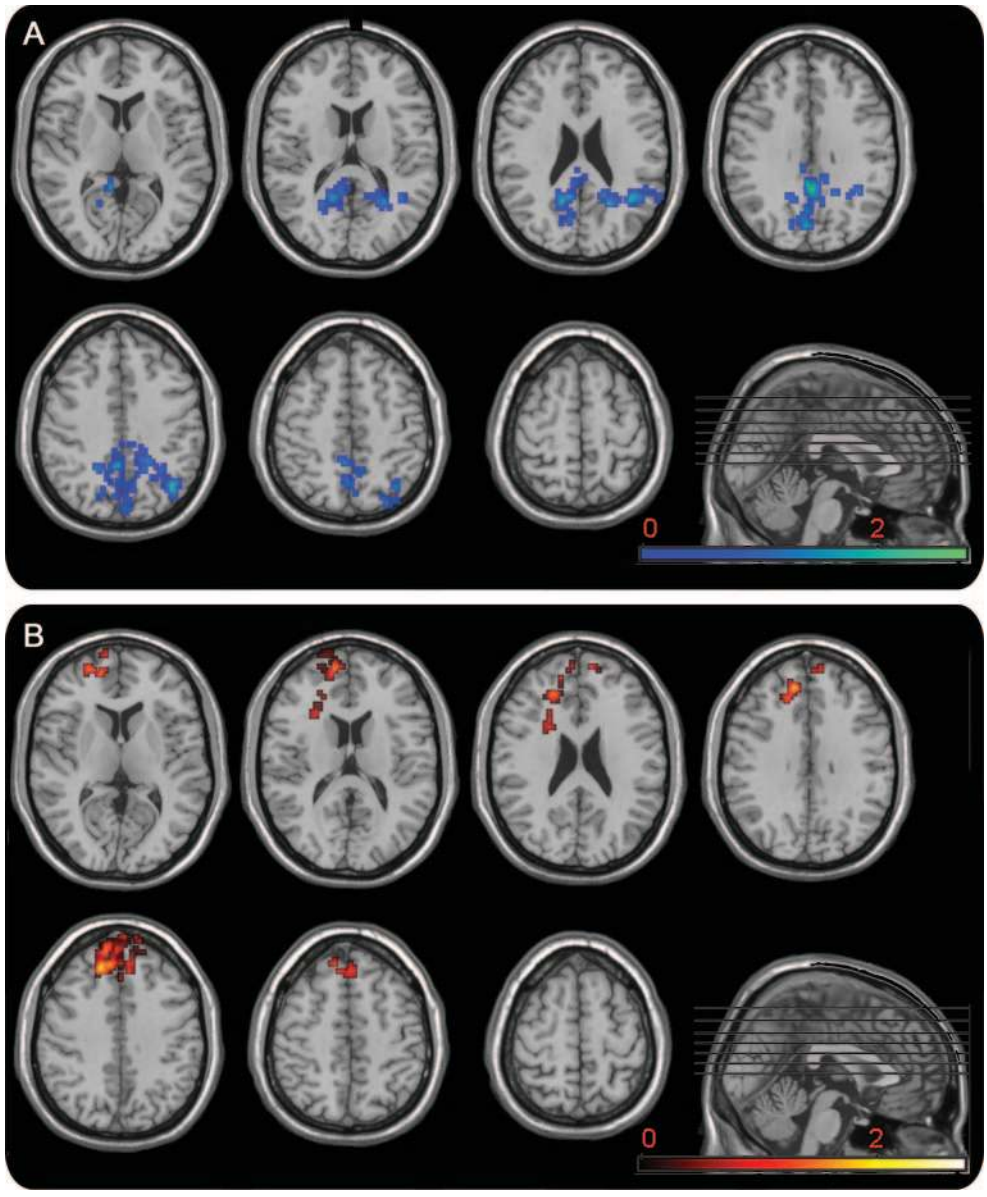

Conjunction analysis between the age cohort regression and the 2-sample *t* test between the subjects with Alzheimer disease (AD) and matched controls using the independent components for the posterior (A) and anterior (B) default mode networks (DMNs). The result for the voxels that showed both age-related decreases in posterior DMN connectivity and decreases in AD are shown in blue (A). The result for the voxels that showed both age-related increases in anterior DMN connectivity and increased connectivity in the AD group are shown in red (B). Results are displayed on a standard template using MRIcro with the color bar coding the *t* score (cluster-corrected $p < 0.05$).

is increased. In addition, atrophy-corrected pDMN connectivity revealed AD increases in connectivity in the posterior cingulate gyrus relative to those in the CN cohort, which was not observed before atrophy correction.

Correlation with STMS in AD and matched control groups. See appendix e-1 and figure e-2 for results.

DISCUSSION In this study of DMN connectivity, we observed an effect of age in a cohort of CN elderly subjects and found that it differs between the aDMN and the pDMN. This is characterized by 3 main effects: 1) the aDMN and pDMN disconnect from each other with advancing age; 2) the pDMN declines in within-network connectivity; and 3) the aDMN has both declines and increases in within-network connectivity. We also investigated the differences in connectivity between a CN cohort matched by age, gender, and education to 28 patients with AD. We found that patients with AD display differences in the aDMN and pDMN connectivity that resemble the age-associated changes in connec-

Figure 4 Alzheimer disease (AD) vs cognitively normal (CN) using seeds

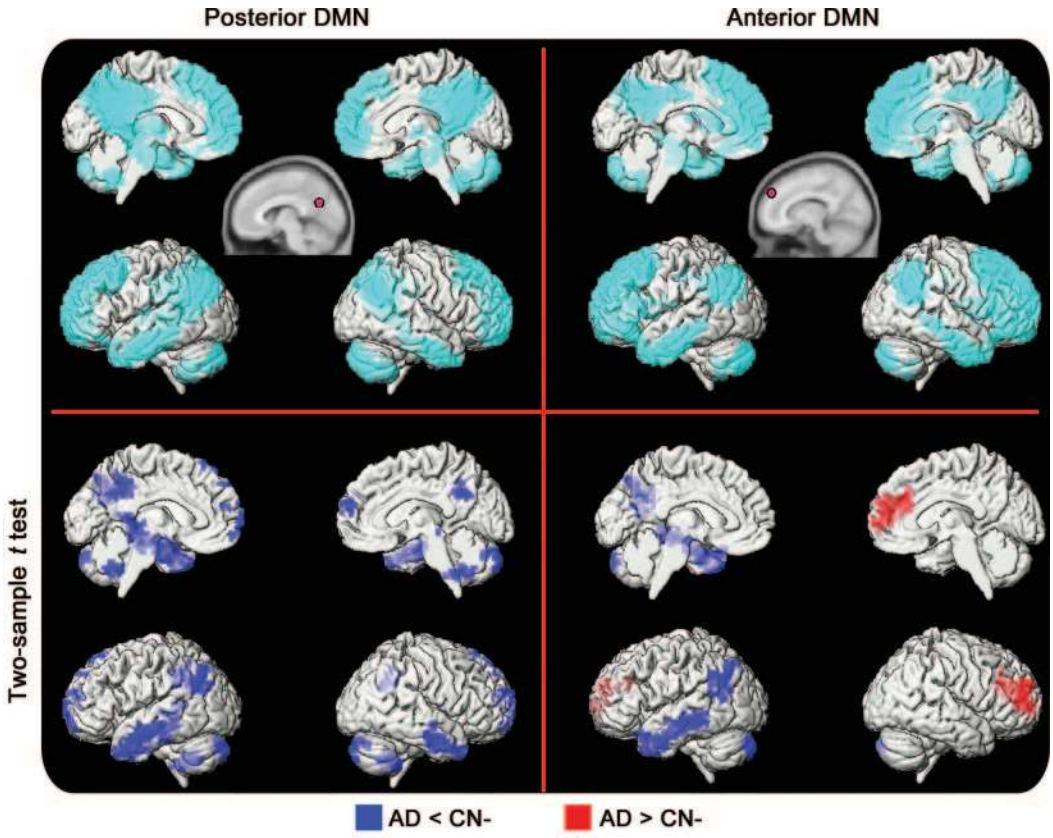

Seed-based analysis of posterior (left) and anterior (right) default mode networks (DMNs) in subjects with AD and matched controls. The spatial extent of the anterior DMN and posterior DMN is displayed in the top row (cyan) using a rendering of a 1-sample *t* test for the entire group (false discovery rate–corrected $p < 0.05$). The seed location and size are approximated in the top row inset (pink circle). Regions displaying greater connectivity in the AD group are in red, and regions displaying less connectivity in AD are in blue (corrected cluster-level $p < 0.05$).

tivity described above. Age-associated connectivity declines in the pDMN are greater in the AD group, whereas the aDMN age-associated connectivity changes in the frontal lobe lose specificity in the AD group, which displayed diffuse frontal lobe increases in connectivity and no decrease. We speculate that this loss of specificity in age-associated frontal lobe changes may be the consequence of prolonged synaptic inefficiency in the brains of individuals more susceptible to developing AD.

Recent work demonstrates that the DMN in older cohorts, such as the one we studied here, has network properties distinct from those in young populations.[4–7] The anterior and posterior portions of the DMN develop greater independence from each other in their respective signal time courses with advancing age, and this phenomenon results in reciprocal DMN changes in anterior and posterior networks.[7] Within-network connectivity declines in the pDMN, whereas the aDMN develops a more independent signal time course from posterior regions and strengthens in within-network connectivity with advancing age in regions of the frontal lobe. If, indeed, resting functional connectivity changes are affected by learning via changes in synaptic plasticity, as has been recently suggested,[23] then age-associated changes in frontal connectivity may be secondary to accumulated plastic changes over a lifetime. This would indicate that age-related synaptic inefficiency over a lifetime can be measured in connectivity studies.

The age effect on the aDMN and pDMN leads to difficulty in selecting the true DMN in older cohorts based on properties of ICN from younger cohorts, which may explain varying reports of ICN abnormalities in AD.[8,9,24–27] If only the pDMN is analyzed (by ICA component selection or posterior seed placement), then the increased frontal lobe connectivity in AD may not be observed. We analyzed both the aDMN and pDMN using a rigorously matched cohort of CN noncarriers of the *APOE* ϵ4 allele and demonstrated connectivity differences using 2 techniques (ICA and seed-based). This result supports the claim that there are differential effects in the pDMN and the aDMN, which are technique-independent.

We do not have measures, such as brain amyloid imaging, of occult AD pathology in our large age cohort, and, therefore, we cannot be certain that the observed age effect on the aDMN and pDMN is not a result of increasing occult AD pathology with advancing age. However, it has been demonstrated that anterior to posterior disconnection occurs independent of amyloid binding measured via Pittsburgh Compound B.[6] Another recent study also demonstrated similar connectivity changes related to *APOE* $\epsilon 4$ carrier status in Pittsburgh Compound B–negative subjects with normal levels of CSF $A\beta_{42}$.[28] In addition, a recent cross-sectional study of aging in a cohort ranging in age from 20s to90s[7] demonstrated that age-associated changes in connectivity appear to accumulate gradually from year to year rather than only in later life when occult AD pathology should begin to be prevalent. Results from these studies argue that subjects at risk for developing AD are more vulnerable to the processes that affect connectivity during normal aging decades before amyloid pathology is present. This line of reasoning is supported by recent studies showing connectivity abnormalities early in life related to *APOE* $\epsilon 4$ allele carrier status.[29]

In our study, the difference in connectivity between the AD and matched CN groups could not be accounted for by differences in gray matter density, which is consistent with previous reports.[30] This supports the view that connectivity abnormalities are not simply a consequence of atrophy. Future work will need to be focused on connectivity and atrophy relationships extending from prodromal states to advanced AD. This will be an important step in integrating TF-fMRI in the biomarker armamentarium. In this regard, seed-based analysis guided by ICA shows promise for making reliable assessments of ICN on an individual subject level. Seed-based analysis (guided by ICA) is not constrained by group properties and reveals medial temporal lobe abnormalities not identified using ICA only (figure 4, figure e-1).

In addition, this study demonstrates that connectivity changes are related to cognitive performance in both the CN and AD groups. We found greater connectivity in the posterior node (a younger pattern of connectivity) in subjects with better performance on the STMS (figure e-2). However, greater connectivity between the anterior node and the frontal lobe (an older and AD pattern of connectivity) was found in subjects with poorer performance on the STMS in both groups. It is not certain whether the poorer performance associated with greater frontal lobe connectivity is a compensatory response to pathology or whether it represents a more proximate event leading to cognitive dysfunction. However, the fact that it is associated with poorer performance in the CN group and is associated with increasing age beginning well before cognitive dysfunction would support the latter. The role of the DMN in cognition is thought to relate to internally directed mental phenomena not immediately related to the external environment,[31] whereas task-positive network regions are more related to processes that involve ongoing interactions with the external environment or bodily milieu.[2] Efficiently moving between these theorized brain states would be important for performing a variety of tasks throughout different cognitive domains surveyed in the STMS. This line of reasoning is consistent with our observation that DMN connectivity patterns are associated with cognitive performance. It should be noted that this study was limited only to changes in the DMN, and future work is needed to investigate whether these findings are specific for the DMN or extend to other ICNs including the task-positive network.

The results of this study support our hypothesis that the DMN abnormalities observed in AD represent an accelerated aging pattern of connectivity compared with that in matched controls. In addition, we have demonstrated that this same pattern is associated with cognitive performance for both subjects with AD and CN subjects.

AUTHOR CONTRIBUTIONS

Dr. Jones: drafting/revising the manuscript, study concept or design, analysis or interpretation of data, contribution of vital reagents/tools/patients, and statistical analysis. Dr. Machulda: drafting/revising the manuscript and study concept or design. Dr. Vemuri: drafting/revising the manuscript, study concept or design, and analysis or interpretation of data. Dr. McDade: drafting/revising the manuscript. Dr. Zeng: acquisition of data. M.L. Senjem: analysis or interpretation of data and contribution of vital reagents/tools/patients. Dr. Gunter: study concept or design, analysis or interpretation of data, acquisition of data, and statistical analysis. S.A. Przybelski: analysis or interpretation of data, acquisition of data, and statistical analysis. Dr. Ramesh: drafting/revising the manuscript, analysis or interpretation of data, and statistical analysis. Dr. Knopman: drafting/revising the manuscript and acquisition of data. Dr. Boeve: drafting/revising the manuscript and acquisition of data. Dr. Petersen: drafting/revising the manuscript and obtaining funding. Dr. Jack: drafting/revising the manuscript, study concept or design, analysis or interpretation of data, acquisition of data, study supervision, and obtaining funding.

DISCLOSURE

Dr. Jones and Dr. Machulda report no disclosures. Dr. Vemuri receives support from the Robert H. Smith Family Foundation Research Fellowship and the NIH. Dr. McDade receives research support from the NIH/NIA–University of Pittsburgh Alzheimer Disease Research Center. Dr. Zeng, M. Senjem, J. Gunter, and S. Przybelski reports no disclosures. Dr. Avula serves as a consultant for Medical Imaging Solutions. Dr. Knopman serves as Deputy Editor for *Neurology*®; has served on a data safety monitoring board for Eli Lilly and Company; has served as a consultant for Elan/Janssen AI; is an investigator in clinical trials sponsored by Elan/Janssen AI, Baxter International Inc., and Forest Laboratories, Inc.; and receives research support from the NIH. Dr. Boeve has served as a consultant to GE Healthcare; receives publishing royalties for *The Behavioral Neurology of Dementia* (Cambridge University Press, 2009); and receives research support from Cephalon, Inc., Allon Therapeutics, Inc., the NIH/NIA, the Alzheimer's Association, and the Mangurian Founda-

tion. Dr. Petersen serves on scientific advisory boards for the Alzheimer's Association, the National Advisory Council on Aging (NIA), Elan/Janssen AI, Pfizer Inc (Wyeth), and GE Healthcare; receives royalties from publishing *Mild Cognitive Impairment* (Oxford University Press, 2003); serves as a consultant for Elan/Janssen AI and GE Healthcare; and receives research support from the NIH/NIA. Dr. Jack serves on scientific advisory boards for Elan/Janssen AI, Eli Lilly & Company, GE Healthcare, and Eisai Inc.; receives research support from Baxter International Inc., Allon Therapeutics, Inc., Pfizer Inc, the NIH/NIA, and the Alexander Family Alzheimer's Disease Research Professorship of the Mayo Foundation; and holds stock/stock options in Johnson & Johnson.

Received February 14, 2011. Accepted in final form July 6, 2011.

REFERENCES

1. Mayeux R. Epidemiology of neurodegeneration. Annu Rev Neurosci 2003;26:81–104.
2. Seeley WW, Menon V, Schatzberg AF, et al. Dissociable intrinsic connectivity networks for salience processing and executive control. J Neurosci 2007;27:2349–2356.
3. Seeley WW, Crawford RK, Zhou J, Miller BL, Greicius MD. Neurodegenerative diseases target large-scale human brain networks. Neuron 2009;62:42–52.
4. Biswal BB, Mennes M, Zuo XN, et al. Toward discovery science of human brain function. Proc Natl Acad Sci USA 2010;107:4734–4739.
5. Damoiseaux JS, Beckmann CF, Arigita EJ, et al. Reduced resting-state brain activity in the "default network" in normal aging. Cereb Cortex 2008;18:1856–1864.
6. Andrews-Hanna JR, Snyder AZ, Vincent JL, et al. Disruption of large-scale brain systems in advanced aging. Neuron 2007;56:924–935.
7. Jones DT, Vemuri P, Machulda MM, et al. Age effect on functional connectivity. Presented at the American Academy of Neurology 62nd Annual Meeting, April 10–17 2010, Toronto, Canada. Abstract.
8. Greicius MD, Srivastava G, Reiss AL, Menon V. Default-mode network activity distinguishes Alzheimer's disease from healthy aging: evidence from functional MRI. Proc Natl Acad Sci USA 2004;101:4637–4642.
9. Wang K, Liang M, Wang L, et al. Altered functional connectivity in early Alzheimer's disease: a resting-state fMRI study. Hum Brain Mapp 2007;28:967–978.
10. Jones DT, Mateen FJ, Lucchinetti CF, Jack CR Jr, Welker KM. Default mode network disruption secondary to a lesion in the anterior thalamus. Arch Neurol 2011;68:242–247.
11. Davis DG, Schmitt FA, Wekstein DR, Markesbery WR. Alzheimer neuropathologic alterations in aged cognitively normal subjects. J Neuropathol Exp Neurol 1999;58:376–388.
12. Roberts RO, Geda YE, Knopman DS, et al. The Mayo Clinic Study of Aging: design and sampling, participation, baseline measures and sample characteristics. Neuroepidemiology 2008;30:58–69.
13. Chao-Gan Y, Yu-Feng Z. DPARSF: a MATLAB toolbox for "pipeline" data analysis of resting-state fMRI. Front Syst Neurosci 2010;4:13.
14. Calhoun VD, Adali T, Pearlson GD, Pekar JJ. A method for making group inferences from functional MRI data using independent component analysis. Hum Brain Mapp 2001;14:140–151.
15. Fox MD, Zhang D, Snyder AZ, Raichle ME. The global signal and observed anticorrelated resting state brain networks. J Neurophysiol 2009;101:3270–3283.
16. Weissenbacher A, Kasess C, Gerstl F, Lanzenberger R, Moser E, Windischberger C. Correlations and anticorrelations in resting-state functional connectivity MRI: a quantitative comparison of preprocessing strategies. Neuroimage 2009;47:1408–1416.
17. Chang C, Glover GH. Effects of model-based physiological noise correction on default mode network anti-correlations and correlations. Neuroimage 2009;47:1448–1459.
18. Cavaglia M, Dombrowski SM, Drazba J, Vasanji A, Bokesch PM, Janigro D. Regional variation in brain capillary density and vascular response to ischemia. Brain Res 2001;910:81–93.
19. Jack CR Jr, Bernstein MA, Fox NC, et al. The Alzheimer's Disease Neuroimaging Initiative (ADNI): MRI methods. J Magn Reson Imaging 2008;27:685–691.
20. Smith SM, Fox PT, Miller KL, et al. Correspondence of the brain's functional architecture during activation and rest. Proc Natl Acad Sci USA 2009;106:13040–13045.
21. Casanova R, Srikanth R, Baer A, et al. Biological parametric mapping: a statistical toolbox for multimodality brain image analysis. Neuroimage 2007;34:137–143.
22. Kokmen E, Smith GE, Petersen RC, Tangalos E, Ivnik RC. The short test of mental status: correlations with standardized psychometric testing. Arch Neurol 1991;48:725–728.
23. Stevens WD, Buckner RL, Schacter DL. Correlated low-frequency BOLD fluctuations in the resting human brain are modulated by recent experience in category-preferential visual regions. Cereb Cortex 2010;20:1997–2006.
24. Rombouts SA, Barkhof F, Goekoop R, Stam CJ, Scheltens P. Altered resting state networks in mild cognitive impairment and mild Alzheimer's disease: an fMRI study. Hum Brain Mapp 2005;26:231–239.
25. Sorg C, Riedl V, Muhlau M, et al. Selective changes of resting-state networks in individuals at risk for Alzheimer's disease. Proc Natl Acad Sci USA 2007;104:18760–18765.
26. Wang L, Zang Y, He Y, et al. Changes in hippocampal connectivity in the early stages of Alzheimer's disease: evidence from resting state fMRI. Neuroimage 2006;31:496–504.
27. Zhang HY, Wang SJ, Xing J, et al. Detection of PCC functional connectivity characteristics in resting-state fMRI in mild Alzheimer's disease. Behav Brain Res 2009;197:103–108.
28. Sheline YI, Morris JC, Snyder AZ, et al. APOE4 allele disrupts resting state fMRI connectivity in the absence of amyloid plaques or decreased CSF A-β42. J Neurosci 2010;30:17035–17040.
29. Dennis NA, Browndyke JN, Stokes J, et al. Temporal lobe functional activity and connectivity in young adult APOE varϵ4 carriers. Alzheimers Dement 2010;6:303–311.
30. Zhou J, Greicius MD, Gennatas ED, et al. Divergent network connectivity changes in behavioural variant frontotemporal dementia and Alzheimer's disease. Brain 2010;133:1352–1367.
31. Raichle ME, MacLeod AM, Snyder AZ, Powers WJ, Gusnard DA, Shulman GL. A default mode of brain function. Proc Natl Acad Sci USA 2001;98:676–682.